Posttensioned Energy Dissipating Connections for Moment-Resisting Steel Frames

Constantin Christopoulos[1]; Andre Filiatrault, M.ASCE[2]; Chia-Ming Uang, M.ASCE[3]; and Bryan Folz[4]

Abstract: The seismic performance of a posttensioned energy dissipating (PTED) connection for steel frames is investigated analytically and experimentally. The PTED connection incorporates posttensioned high-strength bars to provide a self-centering response along with energy dissipating bars that are able to yield in axial tension and compression. The analytical study involves the development of an equivalent iterative sectional analysis procedure to predict the moment-rotation relationship of the PTED connection. Based on this analytical model, a simple design procedure for PTED connections is described. In the experimental study, a cyclic component test was performed on two energy dissipating bars and a cyclic test was conducted on a large-scale exterior beam-to-column PTED connection. The results of the tests show that the PTED test specimen was able to undergo large inelastic deformations without any damage in the beam or column and without residual drift. The proposed analytical model and design procedure were also validated against the experimental results.

DOI: 10.1061/(ASCE)0733-9445(2002)128:9(1111)

CE Database keywords: Steel structures; Steel frames; Energy dissipation; Connections; Post tensioning.

Introduction

Following the unexpected failures of beam-to-column connections in more than one hundred steel moment-resisting frames (MRFs) during the 1994 Northridge, California earthquake, a comprehensive research program—the SAC Joint Venture—was initiated in the United States to investigate and remediate the causes of these failures (SAC 1994). From the results of this investigation, it was concluded that the major cause of these failures was the low plastic rotation capacity of welded connections. In phase I of the SAC Joint Venture, focus was set on procedures for repairing damaged moment connections. A parallel effort was also initiated by the National Institute of Standards and Technology (NIST) and the American Institute of Steel Construction (AISC) to develop effective retrofit procedures. The study lead to a series of innovative concepts to improve the seismic performance of existing MRFs (Gross et al. 1999). In phase II of the SAC Joint Venture, studies on new construction lead to a better understanding of the cyclic behavior of welded and bolted steel moment connections and to the development of more stringent welding practices (FEMA 2000). These new guidelines, however, have raised the fabrication and erection costs of MRFs. Furthermore, even with these enhanced requirements, inelastic deformations as well as residual drifts are expected to occur under seismic loading.

In parallel with the post-Northridge steel research, moment-resisting connections using posttensioning concepts were developed for precast concrete construction (Priestley 1996). A series of innovative beam-to-column connections, combining self-centering characteristics as well as energy dissipation, were proposed. These studies culminated with the cyclic testing of a full-scale five story precast concrete building incorporating posttensioned moment-resisting connections (Priestley et al. 1999). It was demonstrated that the performance of these connections was excellent under simulated seismic loading. The most significant characteristic of these connections was their capacity to ensure small residual drifts through self-centering capabilities, even when significant inelastic transient deformations were mobilized during the cyclic response.

Recently, this posttensioning technology has been extended to concrete shear walls coupled with steel beams (Shen and Kurama 2000) and to steel MRFs (Ricles et al. 2000, 2001). The systems considered in both of these studies incorporate seat angles to dissipate energy and high strength tendons to provide a self-centering restoring force. These connections exhibited similar self-centering and energy dissipation characteristics as the ones developed for the precast concrete systems. While the use of bolted seat angles may be convenient for erection purposes, the evaluation and modeling of these connections under inelastic cyclic action are complex, being highly dependent on geometric considerations and boundary conditions (Shen and Astaneh-Asl 2000).

This paper contributes further to the development of posttensioned steel structures by proposing a steel moment-resisting connection based on the concept of the hybrid precast concrete connection (Stanton et al. 1997). This system incorporates high strength posttensioned steel bars along with energy-

[1]Graduate Student Researcher, Dept. of Structural Engineering, Univ. of California at San Diego, La Jolla, CA 92093-0085. E-mail: cochrist@ucsd.edu

[2]Professor, Dept. of Structural Engineering, Univ. of California at San Diego, La Jolla, CA 92093-0085. E-mail: afiliatrault@ucsd.edu

[3]Professor, Dept. of Structural Engineering, Univ. of California at San Diego, La Jolla, CA 92093-0085. E-mail: cmu@ucsd.edu

[4]Visiting Associate Professor, Dept. of Structural Engineering, Univ. of California at San Diego, La Jolla, CA 92093-0085. E-mail: bfolz@ucsd.edu

Note. Associate Editor: Andrei M. Reinhorn. Discussion open until February 1, 2003. Separate discussions must be submitted for individual papers. To extend the closing date by one month, a written request must be filed with the ASCE Managing Editor. The manuscript for this paper was submitted for review and possible publication on December 20, 2000; approved on January 30, 2002 . This paper is part of the ***Journal of Structural Engineering***, Vol. 128, No. 9, September 1, 2002. ©ASCE, ISSN 0733-9445/2002/9-1111–1120/$8.00+$.50 per page.

J. Struct. Eng. 2002.128:1111-1120.

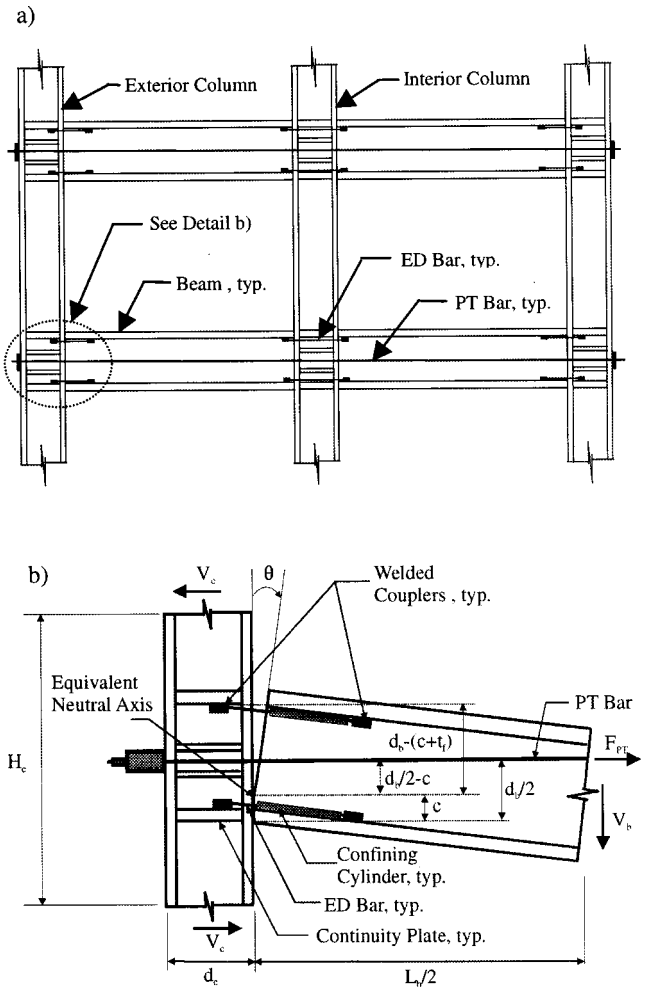

Fig. 1. Concept of posttension energy dissipating steel connection: (a) steel frame with posttension energy dissipating connections; (b) geometric configuration and free-body diagram of exterior posttension energy dissipating connection

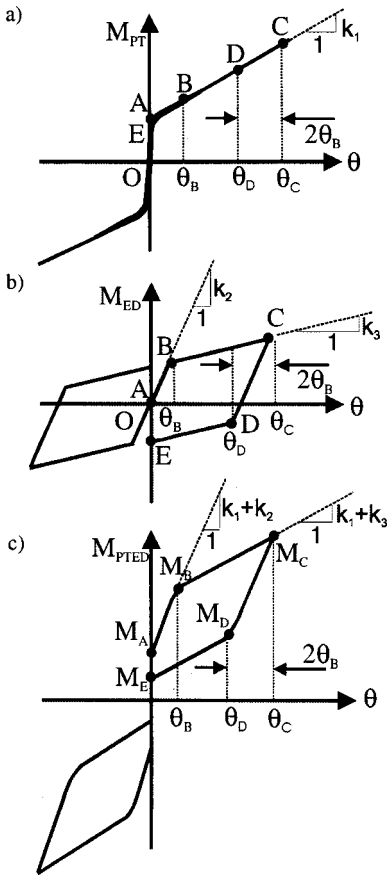

Fig. 2. Idealized hysteretic behavior of posttension energy dissipating beam-to-column connection: (a) contribution of posttension bars; (b) contribution of energy-dissipating bars; and (c) moment-rotation relationship of posttension energy dissipating connection

dissipating (ED) bars. These ED bars, when inserted in steel cylinders to limit buckling, are able to develop stable inelastic axial deformations in both tension and compression. Numerical and experimental results presented in this study show that this connection is capable of achieving stiffness and strength characteristics comparable to a traditional welded moment-resisting connection. In addition, the connection can be designed to provide a sufficient amount of energy dissipation per cycle. Results from nonlinear time-history dynamic analyses on hysteretic self-centering single-degree-of-freedom systems have indicated that the seismic response of these systems can be similar to the response of elastoplastic hysteretic systems by adjusting their ED characteristics (Christopoulos 2002). This structural behavior is achieved without introducing inelastic deformations in the beam or column and without residual drift.

Proposed Posttensioned Steel Moment-Rresisting Connection

The geometric configuration of a frame incorporating the proposed posttensioned energy dissipating (PTED) steel connection is shown in Fig. 1(a). The detail of an exterior beam-to-column PTED connection is shown in Fig. 1(b). The posttension (PT) force F_{PT} is provided by two high strength bars located at mid-depth of the beam, one on each side of the web. Four symmetrically placed ED bars are also included in the connection to provide energy dissipation under cyclic loading. These ED bars are threaded into couplers which are welded to the inside face of the beam flanges and to the continuity plates in the column. Holes are introduced in the column flange to accommodate the PT and ED bars. To prevent the ED bars from buckling in compression under cyclic loading, they are inserted into confining steel cylinders that are welded to the beam flanges. The ED bars are initially stress-free since they are introduced into the connection after the application of the PT force.

For an interior PTED beam-to-column connection, the PT bars pass through the interior column and are anchored to the exterior columns of the frame, as illustrated in Fig. 1(a). Also, the couplers for the four ED bars are field welded to the flanges of the two framing beams. The proposed PTED connection relies on the PT force to maintain contact between the beam and the column. Nonlinear elastic action is introduced by a gap opening at the beam-to-column interface, as shown in Fig. 1(b). Inelastic action takes place through yielding of the ED bars.

Under cyclic loading the resulting moment-rotation [rotation being defined as the gap opening angle θ as shown in Fig. 1(b)] hysteretic response developed at the beam-to-column interface by the PT bars ($M_{PT}-\theta$), the ED bars ($M_{ED}-\theta$), and by the combination of PT and ED bars ($M_{PTED}-\theta$) are shown in Fig. 2. The

J. Struct. Eng. 2002.128:1111-1120.

total moment in the connection, M_{PTED}, can be obtained by summing the moment contributed by the PT bars, M_{PT}, and the moment developed by the ED bars, M_{ED}

$$M_{PTED}=M_{PT}+M_{ED} \tag{1}$$

This combination of moment-rotation relations results in a *flag-shaped* hysteresis [see Fig. 2(c)], in which energy is dissipated while the system retains its self-centering capabilities. When a negative (hogging) bending moment occurs at the beam-to-column interface as shown in Fig. 1(b), the PTED connection behaves elastically as long as full contact is maintained between the beam and the column. To this point, the precompression provided by the PT force is sufficient to maintain contact between the beam and column over the full depth of the beam. Therefore, no gap opening takes place between point O and point A in Fig. 2.

The PT force controls the magnitude of the bending moment M_A beyond which a gap opening exists between the beam and the column. When M_A is reached, a gap opens and the rotational stiffness of the PTED connection is provided by the elastic stiffness of both top ED bars and the PT bars (point A to point B in Fig. 2). Note that the behavior of the connection now becomes nonlinear elastic due to the opening of the gap. This nonlinear elastic behavior continues until a bending moment M_B is reached. This moment is associated with the tensile yield capacity of the top ED bars and is given by:

$$M_B=M_A+(k_1+k_2)\theta_B \tag{2}$$

where k_1=elastic rotational stiffness provided by the PT bars; k_2=elastic rotational stiffness provided by the top ED bars; and θ_B=rotation at which tensile yielding of the top ED bars is initiated.

Under continued loading, the rotational stiffness of the PTED connection is provided by the elastic stiffness of the PT bars and by the postyield stiffness of the ED bars (point B to point C in Fig. 2). Again, the behavior of the connection is nonlinear elastic due to the continued opening of the gap. This behavior is maintained until the maximum rotation in the cycle θ_c is achieved. The corresponding moment developed in the connection M_C is given by

$$M_C=M_B+(k_1+k_3)(\theta_C-\theta_B) \tag{3}$$

where k_3=the postyield rotational stiffness provided by the top ED bars.

Upon reversing the bending direction, the PTED connection exhibits a nonlinear elastic stiffness until the compression yield capacity of the top ED bars is reached (point C to point D in Fig. 2). At that point, the rotation of the connection θ_D is given by

$$\theta_D=\theta_C-2\theta_B \tag{4}$$

The bending moment at that new yield point M_D is given by

$$M_D=M_C-(k_1+k_2)(2\theta_B) \tag{5}$$

Note that this nonlinear elastic behavior is possible only if the top ED bars are prevented from buckling in compression.

During the compression yielding of the top ED bars, the PTED connection exhibits a nonlinear elastic stiffness until full contact is re-established between the beam and the column (point D to point E in Fig. 2). The corresponding bending moment is given by

$$M_E=M_D-(k_1+k_3)\theta_D=M_D-(k_1+k_3)(\theta_C-2\theta_B) \tag{6}$$

As shown in Fig. 2, the behavior of the PTED connection is symmetric in the opposite positive half cycle of loading, in which tensile and compression yielding of the bottom ED bars are mobilized. At the end of the cycle, when full contact is re-established between the beam and the column ($\theta=0$), both ED bars develop their yield capacity in compression.

Note that full self-centering of the PTED connection occurs provided that M_E is positive at the end of the first half cycle. Substituting Eqs. (2), (3), and (5) into Eq. (6) results in the following condition to ensure full self-centering of the connection:

$$M_A \geqslant (k_2-k_3)\theta_B \tag{7}$$

Eq. (7) can be used as a necessary condition in the design of the PT and ED bars.

Conceptually, with a properly proportioned PT force, no physical shear connection would be required between the beam and the column. Shear transfer could be adequately provided through Coulomb-type friction at the beam-to-column interface. A special treatment of the contact surfaces, such as sand blasting, would further increase the friction coefficient. However, considering the unknown reliability of such a friction shear transfer mechanism at the beam-to-column interface, further experimental studies are required to verify this concept. Alternative modes of shear transfer could be used, as long as they do not interfere with the moment-rotation characteristics of the PTED connection. Such alternatives could include horizontally slotted shear tabs connected to the web of the beam or long and flexible seat angles below the beams that are able to deform without developing substantial moment capacity. The dowel action of the ED and PT bars could also provide an alternate shear transfer mechanism in case of a loss of PT force between the beam and the column.

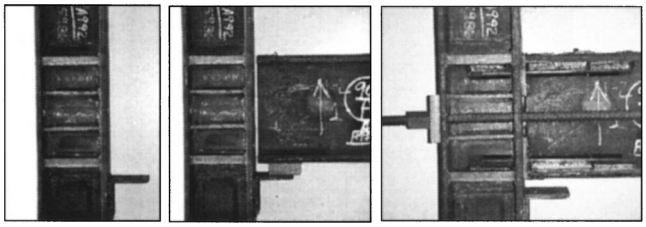

Fig. 3. Erection sequence for posttension energy dissipating connection: (a) column with erection seat angle; (b) beam on shim atop seat angle; and (c) installation of contact plates, posttension bars and energy dissipating bars and removal of shim

Erection Sequence of Frames with Posttensioned Energy Dissipating Steel Connections

Fig. 3 illustrates a possible practical erection sequence for PTED beam-to-column connections. First, the columns are erected [Fig. 3(a)]. The columns include shop-welded horizontal stiffeners and seat angles to facilitate the subsequent erection of the beams. The beams are then installed and aligned on a shim atop of the seat angles [Fig. 3(b)]. Temporary erection side angles shop welded to the columns and bolted to the beams could be used to laterally support the beams. Contact plates are then welded at the end of each beam to fill the gap between the beam and the column. These plates can be inserted from the top and both sides of the beam, without interfering with the shim atop of the seat angle. This gap is intentionally provided to facilitate the placement of the beams and to accommodate construction tolerances. The PT

J. Struct. Eng. 2002.128:1111-1120.

and ED bars are then installed [Fig 3(c)]. Upon completion of the connections, the shims are removed to allow the beams to rotate freely during seismic loading.

Analytical Model of Posttensioned Energy Dissipating Steel Connection

An analytical procedure to predict the complete monotonic moment-rotation relationship of a PTED steel connection is outlined in this section. As long as the moment is below M_A (see Fig. 2), the PTED connection behaves as a fully restrained moment connection as defined by AISC (1993). Up to this level of loading, the PT force ensures full contact between the beam and the column. When the moment M_A is exceeded, a gap begins to form between the beam and the column. Tensile strains are thus induced in the ED bars crossing the gap. Additional tensile strains are also superimposed on the initial posttensioning strains in the PT bars. As illustrated in Fig. 1, the tip of the gap opening, located at a distance c from the bottom of the compression flange of the beam, can be considered as the equivalent neutral axis of the connection interface. After a gap opens, strain compatibility is lost between the end of the beam and the flange of the column. A trilinear moment-rotation idealization was first proposed by Priestley and Tao (1993) and a fiber model was later developed by El-Sheikh et al. (1998) to model precast posttensioned concrete connections exhibiting similar mechanical characteristics. This fiber model fully characterizes the moment-rotation behavior of this type of connection but requires considerable analytical and computational effort, making it impractical for design purposes. Pampanin et al. (1999) proposed a simple iterative beam sectional procedure to evaluate the behavior of precast posttensioned concrete connections incorporating unbonded tendons. A similar beam sectional approach is adopted herein to model the moment-rotation characteristics of the proposed PTED steel connection.

For a given gap opening angle θ and neutral axis position c, the strains developed in the PT bars ε_{PT} and in the ED bars ε_{ED} are given by

$$\varepsilon_{PT}=\varepsilon_{in}+\left[\frac{(d_b/2-c)\theta}{L_{PT}}\right]\left(1-\frac{A_{PT}}{A_b}\right) \tag{8}$$

$$\varepsilon_{ED}=\frac{[\theta(d_b-t_f-c)]}{L_{ED}} \tag{9}$$

where d_b=depth of the beam; ε_{in}=initial strain in the PT bars; t_f=thickness of the beam flanges; L_{PT}=length of the PT bars; L_{ED}=length of the ED bars; and A_{PT} and A_b=cross-sectional areas of the PT bars and beam, respectively. The ratio A_{PT}/A_b in Eq. (8) accounts for the fact that when the PT force is increased as a result of the gap opening, the beam is subjected to additional axial compression and shortens further. This additional shortening of the beam reduces the PT force. Furthermore, it is assumed that the normal compressive strains over the contact region between the beam and the column vary linearly from zero at the equivalent neutral axis to ε_{max} at the extreme fiber.

Eqs. (8) and (9) are only valid for a beam that can experience free elongations, such as the one tested in this study. These equations can be modified to take into account the restraint that the columns would have on the axial deformations of the beams in a frame system.

The relationship between ε_{max} and the position of the neutral axis c is obtained through member compatibility by using an analogy with a classical welded connection and is assumed to be

$$\varepsilon_{max}=c\left(\frac{\theta}{d_b}+\alpha\phi_y\right) \tag{10}$$

where ϕ_y=yield curvature of the beam and α=calibration factor obtained numerically by requiring that the neutral axis be located at the top flange of the beam ($c=d$) for a very small gap opening angle. Further details on this formulation can be found in Pampanin et al. (1999).

This analytical procedure has been implemented in a computer program to construct the complete moment-rotation relationship of a PTED steel connection. The steps required to compute the moment M_{PTED} corresponding to a given gap opening angle θ are:

1. Assume a position of the neutral axis c,
2. Compute the axial strain ε_{PT} in the PT bars using Eq. (8), the axial strain ε_{ED} in the ED bars using Eq. (9), and the linear normal strain profile in the compression zone characterized by the maximum normal strain ε_{max} by Eq. (10) at the compression flange of the beam and zero at the neutral axis,
3. Compute the resulting normal stresses using the individual stress–strain relationships for each of the components,
4. Integrate the normal stresses over the respective areas to obtain the corresponding normal force in each component,
5. Sum the normal forces and check for horizontal equilibrium,
6. Iterate over the position of the neutral axis c by returning to step 1. until horizontal equilibrium is satisfied, and
7. Compute the moment M_{PTED} associated with the corresponding gap opening angle θ once equilibrium is satisfied.

The procedure is repeated for increasing values of the gap opening angle θ until the complete monotonic moment-rotation relationship is determined. This procedure can be further extended to define a cyclic model of the connection. For each value of gap opening angle, the moment contributions of the PT bars M_{PT} and of the ED bars M_{ED} are computed (see Fig. 2). Separating the total moment M_{PTED} into these two contributions allows for the definition of two equivalent rotational springs at the connection level. As illustrated in Fig. 2, the rotational spring modeling the PT force exhibits a nonlinear elastic behavior, while the rotational spring modeling the ED bars displays a bilinear hysteretic behavior. Rather than fitting the entire moment-rotation characteristic to a single hysteretic rotational spring element, this approach allows for a more realistic modeling of the cyclic behavior since the PT bars are not expected to undergo any inelastic action while the ED bars undergo significant cyclic inelastic deformations.

Design of Posttensioned Energy Dissipating Experimental Specimen

Once the moment-rotation characteristics of the connection are obtained for any given rotation, the resulting forces in the beam and column can be statically determined. Fig. 1(b) shows the free-body diagram of the PTED beam-to-column connection for a target gap opening angle $\theta=\theta_t$, causing a target moment M_t at the column face. Note that it is assumed that this target moment is known and has been determined based on the required global lateral capacity of the building at the design drift level. Further work is needed to provide design guidelines for the selection of M_t and is not addressed herein.

The shear force V_b in the beam and the shear force V_c in the column can be expressed in terms of the moment in the connection M_t

$$V_b=\frac{2M_t}{L_b} \tag{11}$$

J. Struct. Eng. 2002.128:1111-1120.

$$V_c = \frac{M_t}{H_c}\left(1 + \frac{d_c}{L_b}\right) \tag{12}$$

where H_c=interstory height measured from the expected inflection points assumed at midstory height; L_b=clear span of the beam; and d_c=depth of the column. Note that Eqs. (11) and (12) also assume an inflection point at midspan of the beam.

Using capacity design, all components of the beam-to-column connection with the exception of the ED bars must remain elastic. At the target rotation, it can be assumed that the neutral axis is located at a distance $c = t_f$ from the edge of the compression flange. As will be shown later, this assumption agrees well with the experimentally measured position of the neutral axis for large rotations ($\theta > 0.015$ rad). Based on this assumption, the design of each component of the PTED connection can be performed as follows:

1. The PT bars must always remain elastic. The PT bars are positioned at mid-depth of the beam where the strain increase under cyclic loading is minimized. The condition for which the strain ε_{PT} in the PT bars remains below the yielding strain ε_{yPT} of the steel can be verified through Eq. (8) for $c = t_f$.
2. The bending moment generated by the axial forces in the ED bars about the equivalent neutral axis must always be smaller than the corresponding bending moment generated by the axial forces in the PT bars to ensure full self-centering of the connection. This condition is given by Eq. (7). For design purposes, this requirement can be expressed more conveniently by considering the sum of the moments about the assumed equivalent neutral axis, which results in the following condition:

$$\frac{F_{ED}}{F_{PTin}} \leq \frac{(d/2 - t_f)}{(d - 2t_f)} \tag{13}$$

where F_{ED}=total force developed in the ED bars at the target rotation including strain hardening effects and F_{PTin}=initial PT force. Eq. (13) corresponds to point E in Fig. 2 when the beam re-establishes full contact with the column. At that point, both pairs of ED bars on the top and bottom of the beam are yielding in compression and the PT bars return to their initial length.

3. The beam must be designed as a beam-column member for the combined effect of gravity loads, PT force and total bending moment, M_{PTED}, applied at the face of the column.
4. Shear must be carried by the beam along its span, and transferred by friction through the contact surface at the beam-to-column interface. The web capacity of the beam is simply checked against the maximum shear in the beam when the maximum moment is produced at the connection level. The shear transfer from the beam to the column is provided by Coulomb-type friction mobilized by the PT force. Current steel design provisions (AISC 1993) recommend a friction coefficient of $\mu = 0.33$ for a steel-to-steel interface. This friction coefficient can be increased to 0.55 if the contact surfaces are sand blasted. The two conditions that must be satisfied in order to ensure adequate transfer of the shear force by friction are given by

$$\mu F_{PT} \geq \frac{2M_t}{L_b} + V_D \quad \text{for } \theta = \theta_t \tag{14}$$

$$\mu(F_{PT} - 2F_{ED}) \geq V_D \quad \text{for } \theta = 0 \tag{15}$$

where V_D=shear induced by the design gravity loads acting on the beam. Eq. (14) expresses the PT force required to provide sufficient shear strength at the target rotation. Note that the forces in the ED bars do not appear in this equation. It is assumed, as a worst case scenario, that the ED bars located in the compression zone of the section have yielded in tension in a previous cycle and have developed their compressive yield strength when the gap closes back. Therefore, the forces in the ED bars located in the tension and compression zones of the section cancel each other out. Eq. (15), on the other hand, expresses the PT force required to provide sufficient shear resistance at the beam-to-column interface when the beam is in full contact with the column (i.e., zero rotation), after the ED bars located both at the top and bottom of the beam section have yielded in previous cycles. The value of F_{ED} in Eq. (15) is the maximum inelastic compressive force developed in the ED bars. Note that the dowel effect provided by the ED and PT bars is not included in Eqs. (14) and (15).

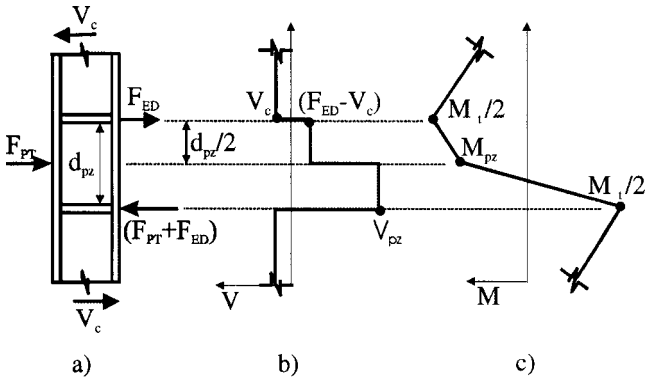

Fig. 4. Column pane zone at exterior posttension energy dissipating beam-to-column connection: (a) horizontal forces; (b) shear forces; and (c) bending moments

5. As shown in Fig. 4, the maximum shear force in the panel zone of the column is given by

$$V_{pz} = F_{PT} + F_{ED} - V_c \tag{16}$$

Note that because of the presence of the PT force, the shear force is not constant through the column panel zone. The panel zone shear strength can be computed from the formula given by the AISC seismic provisions (1997). Note also that the shear force distribution given in Fig. 4 and used in Eq. (16) is valid only for an exterior beam-to-column connection, but can be easily extended to an interior connection.

6. The flexural design of the column is based on the weak beam-strong column philosophy. For this purpose, two potential critical sections must be considered. As shown in Fig. 4, the first critical section is located outside the panel zone where the maximum moment in the column is $M_t/2$. The second critical section is located inside the panel zone where a bending moment M_{pz} is induced at the location of the PT bars. This panel zone bending moment occurs because of the nonuniform shear distribution in the panel zone and is given by

$$M_{pz} = \tfrac{1}{2}[M_t - (F_{ED} - V_c)d_{pz}] \tag{17}$$

where d_{pz}=depth of the panel zone. Note that this critical section inside the panel zone may govern the flexural design of the column. The introduction of holes in the column flanges to accommodate the PT bars results in a reduction in the flexural capacity of the column.

J. Struct. Eng. 2002.128:1111-1120.

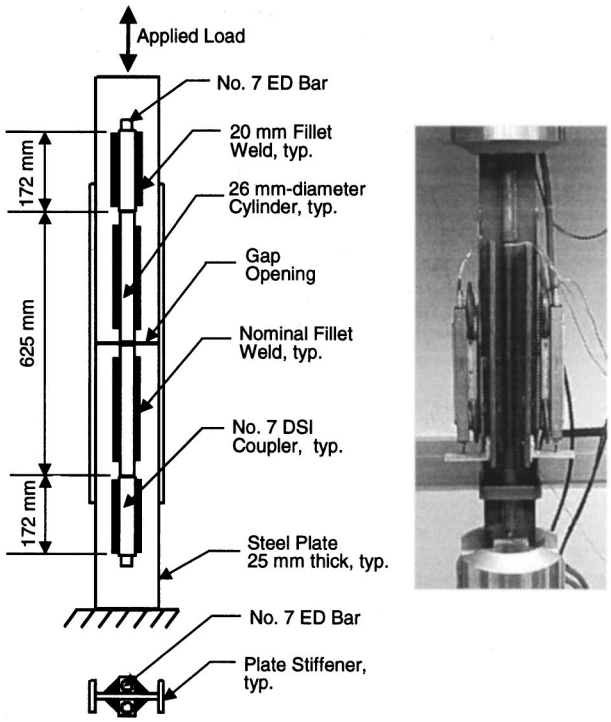

Fig. 5. Experimental setup for component testing of energy dissipating bars

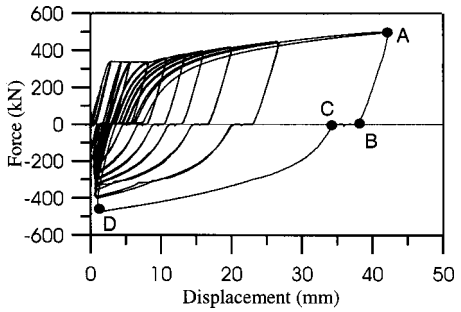

Fig. 6. Cyclic response of component test specimen (two energy dissipating bars)

Experimental Evaluation

A cyclic test was carried out on a large-scale exterior beam-to-column connection to investigate the performance of the proposed PTED connection and to assess the validity of the analytical model and of the design procedure presented herein. In order to verify the behavior of ED bars connected by welded couplers and confined by steel cylinders, a component test was first carried out.

Component Testing of Energy Dissipating Bars

The component testing of the ED bars had three main objectives: (1) to assess the tension-compression cyclic behavior of the ED bars, (2) to verify that the welded couplers could develop the full axial capacity of the ED bars, and (3) to evaluate the effectiveness of the confining cylinders in limiting buckling of the ED bars.

Fig. 5 shows the experimental setup used for the component testing of the ED bars. Two 25 mm thick steel plates were used to represent the beam flange and the continuity plates of the column. These plates were rigidly clamped in a universal testing machine to prevent in-plane rotation of the test specimen under loading. The gap opening that would occur in the PTED connection was simulated by a similar gap between the two steel plates. Each loading cycle consisted of separating the plates by applying a tension force to the system. Once the target opening gap was reached, the load was reversed until the displacement between the two plates is brought back to zero. To avoid eccentricity in the test setup, two ED bars were tested simultaneously.

The ED bars used in the test were 22 mm diameter No. 7 Dywidag System International (DSI) threaded bars with a nominal yield stress of 400 MPa. These bars, having an unbonded length of 625 mm, were threaded into couplers that were welded to each steel plate. To limit buckling of the ED bars in compression, confining structural steel cylinders were introduced. Each cylinder had a wall thickness of 3.5 mm and an interior diameter of 26 mm, which allowed free axial deformation of the ED bars. These cylinders were welded to the steel plates.

The cyclic response of the component test specimen is shown in Fig. 6. The first few cycles were applied in the elastic range of the bars. When the bars yielded in tension and a substantial gap opened between the plates, three different regions characterized the load reversal from the peak displacement to the zero gap position. These three regions are identified by points A to D on the last unloading cycle in Fig. 6. The first region is characterized by an elastic unloading of the system (point A to point B in Fig. 6). In the second region (point B to point C in Fig. 6), a slip in the coupler-bar connection causes a small flat force–displacement response when the load in the ED bars transits from tension to compression. As the ED bar yields significantly in tension, permanent deformations occur in the threaded portion of the bar, which results in a slack in the coupler-bar connection upon reversal of the load. One mean of eliminating this slip would be to use tapered ED bars for which their threaded portions would remain in the elastic range. Finally, the third region (point C to point D in Fig. 6) is characterized by the restrained inelastic buckling of the ED bars inside the confining cylinders.

Despite the inelastic buckling of the ED bars inside the confining cylinders and the small slip in the couplers during loading reversal, the hysteretic behavior of the system is stable with good energy dissipation characteristics. The unbonded length of the ED bars should be selected for the PTED connection such that at the target gap opening angle, the axial strain induced in the ED bars falls within the high-energy dissipating loops (displacement larger than 20 mm in Fig. 6). Note that the maximum displacement (43 mm) achieved in the component test corresponds to a gap opening generated by an interstory drift of 10% in the PTED connection tested herein, as described next. The strain induced in the ED bars at this displacement is only 20% of the ultimate strain of the steel. Note that in a PTED connection, the ED bars might be experience stress concentration from their rotation near the couplers. Further experimental work is required to investigate this phenomenon. Nevertheless, from the results obtained from the component testing, it was concluded that the assembly encompassing ED bars, welded steel couplers, and confining cylinders exhibited good energy dissipating response and could be incorporated in the proposed PTED connection.

Large-Scale Connection Test

Based on the procedure described earlier, a large-scale exterior beam-to-column PTED connection specimen was designed. The target gap opening angle was set equal to 0.04 rad, which corre-

J. Struct. Eng. 2002.128:1111-1120.

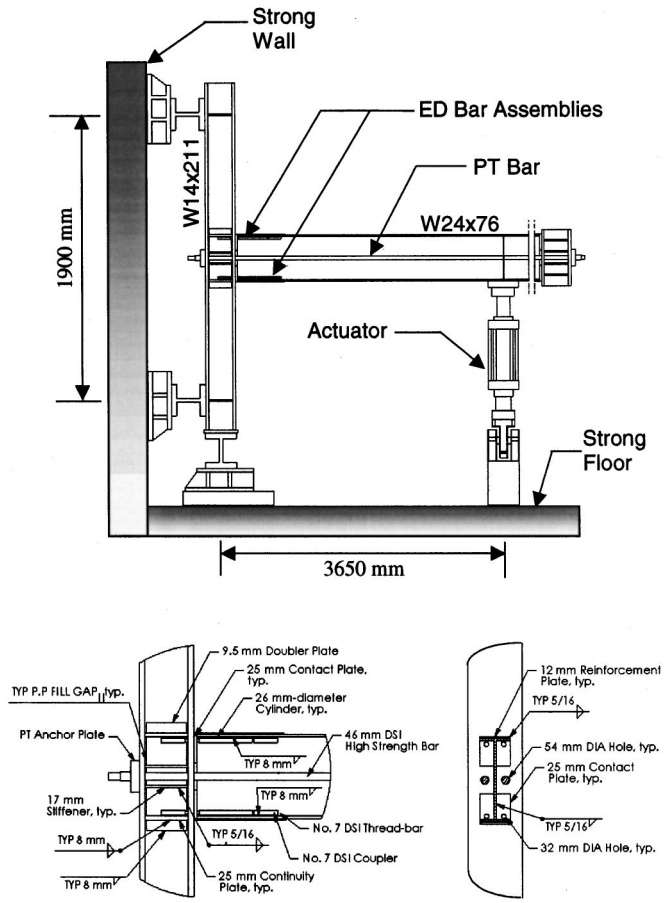

Fig. 7. Experimental setup for posttension energy dissipating connection test

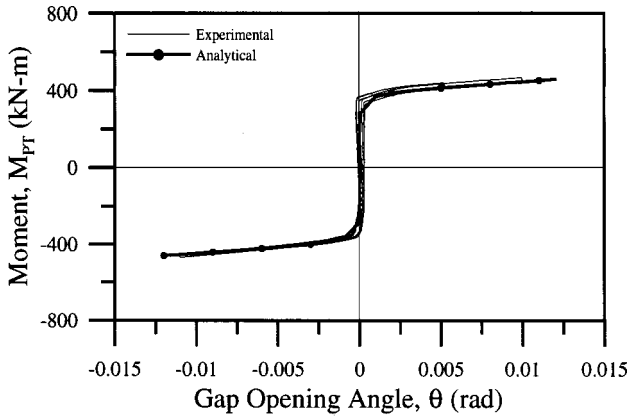

Fig. 8. M_{PT} relationship of connection with posttension bars only

sponds to an interstory drift of approximately 5% for the test specimen. Once the beam section was selected, the other components of the PTED connection were obtained by Eqs. (11)–(17). The design process is iterative since these equations can be satisfied for various combinations of the PTED connection components.

Fig. 7 illustrates the resulting exterior PTED beam-to-column connection tested under quasistatic cyclic loading. The beam and column sections considered were W24×76 and W14×211, respectively. Both the beam and the column were A992 steel with a nominal yield strength of 345 MPa. The PT force was provided by two 46 mm diameter DSI high strength bars with a nominal ultimate strength of 1030 MPa, positioned at middepth of the beam. Although the simulated beam shear was applied by an actuator positioned at midspan along the beam, the PT bars were anchored at a distance corresponding to the full span of the beam (7,300 mm). The beam flanges were reinforced with 12 mm thick Grade 50 plates to reduce the potential yielding of the flanges at the compression contact region. The length of these reinforcing plates is selected such that they end at a location where the beam section alone can safely carry the bending moment and axial load induced at that location when the target gap opening angle, θ_t, is reached. The column web in the panel zone was reinforced by two 9.5 mm thick grade 50 doubler plates to provide additional shear strength. Grade 50 continuity plates, 25 mm thick, were fillet welded on the column web at the level of the beam flanges to provide an adequate transfer of compression forces from the beam to the column. Additionally, 17 mm thick grade 50 horizontal stiffeners were also positioned near the center of the panel zone where the PT bars were anchored. Contact plates, 25 mm thick, were fillet welded to the end of the beam to provide a continuous contact surface between the beam and column flange.

The contact surfaces of the column flange and beam contact plates were sand blasted to increase the friction coefficient. Four 22 mm diameter (No. 7) DSI threaded bars with a nominal yield strength of 400 MPa were used for the ED bars. The unbonded length of each ED bar was 550 mm.

After the beam was shored and aligned with the column, each PT bar was posttensioned to a force of 655 kN. Before the ED bars were installed, the specimen was subjected to a series of displacement cycles to investigate the nonlinear elastic behavior provided by the PT force alone. Fig. 8 shows the moment-rotation response of the connection when only the PT bars are present. The nonlinear elastic characteristic and the recentering capability of the connection are evident. Fig. 8 also shows the response of the connection predicted by the analytical model described earlier. The predictions of the analytical model are in good agreement with the experimental results.

After this initial evaluation, the PTED connection was completed by welding the couplers and confining cylinders in place and threading in the ED bars as shown in Fig. 7. The PTED steel connection was then subjected to the testing protocol developed for the SAC steel project (Clark et al. 1997) up to a maximum interstory drift of 4%. Fig. 9 shows a photograph of the PTED test specimen at this maximum interstory drift. Even at this large drift level, no noticeable damage was observed in the PTED connection; the beam compression flanges did not buckle, no inelastic deformations occurred in the column panel zone or the column flanges, and no slip was observed across the beam-to-column interface. Furthermore at the end of the test, no residual drift was observed, indicating that the combination of ED and PT bars resulted in a PTED connection that performed as expected. None of the ED bars fractured during the test. The ED bars were able to adequately handle the supplementary stresses induced by their rotation near the couplers.

The experimental force–interstory drift response of the system along with the loading protocol are shown in Fig. 10. A numerical prediction of this response is also shown in Fig. 10. The test specimen exhibits a *flag-shaped* hysteresis. Even at the maximum interstory drift of 4%, full self-centering capability is achieved by the PTED connection. The linear region in Fig. 10 corresponds to the contributions of the elastic flexural and shear deformations of the beam, column and panel zone to the interstory drift. Notice-

J. Struct. Eng. 2002.128:1111-1120.

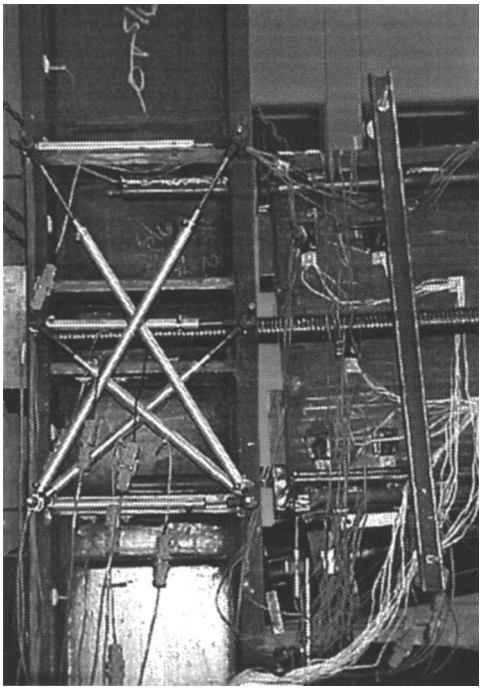

Fig. 9. Posttension energy dissipating connection at 4% interstory drift

able reduction in stiffness during unloading can be observed for drift levels greater than 2%. This reduction of stiffness can be attributed to the slip between the ED bars and the couplers during load reversals and to the yielding of the contact steel between the beam and the column. As shown in Fig. 10, the numerical cyclic model of the PTED connection, based on two parallel rotational springs as discussed earlier, closely predicts the test results. This prediction was obtained by combining available hysteretic models within the general inelastic dynamic analysis program *RUAUMOKO* (Carr 2000).

Fig. 11(a) compares the experimental moment-rotation of the PTED connection with the predictions of the analytical model described earlier. Note that the elastic contribution of the measured response in Fig. 10 is removed from Fig. 11(a) in order to obtain the moment-rotation relationship. The envelope of the moment-rotation is predicted well by the model. The measured bending moment corresponding to the yield capacity of the ED bars is equal to 580 kN m. This value corresponds to 58% of the nominal yield moment of the W24×76 beam section used in the test specimen. The maximum bending moment developed by the

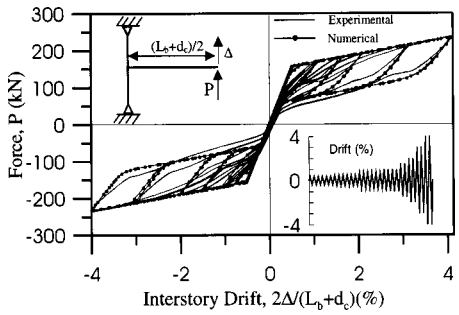

Fig. 10. Experimental and numerical force-interstory drift response of test specimen

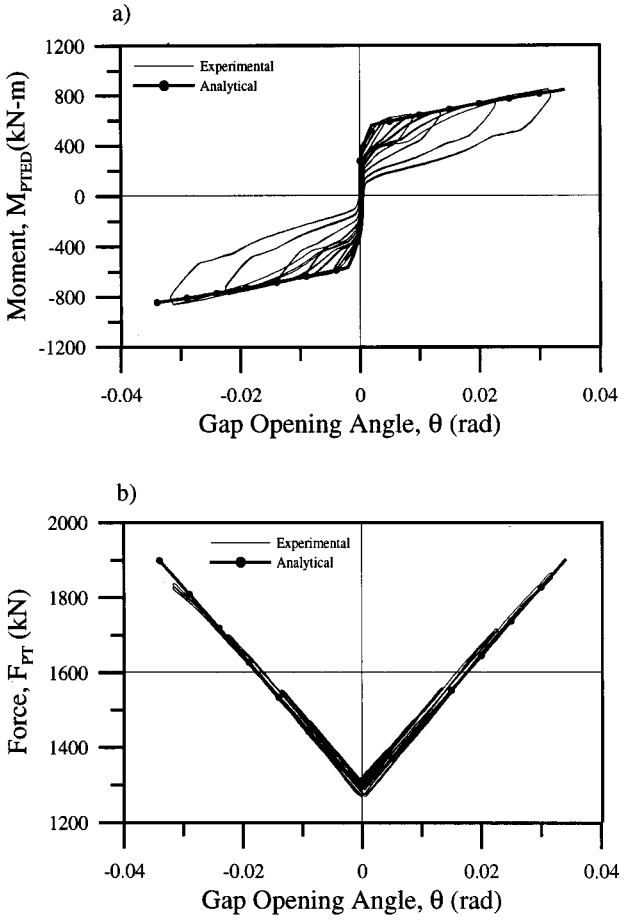

Fig. 11. Response of posttension energy dissipating connection: (a) M_{PTED}—θ and (b) F_{PT}—θ

connection at an interstory drift of 4% is equal to 870 kN m. This value corresponds to 76% of the nominal plastic moment of the same beam section. In a design situation, these equivalent strength values can be adjusted by proper selections of the ED bars, PT bars and initial PT force, as discussed earlier. Fig. 11(b) compares the PT force-rotation relationship measured during the test with the analytical model prediction. The PT force was measured during the test with load cells positioned at the end of the PT bars. The model prediction uses Eq. (8) to compute the PT force corresponding to a gap opening angle. The analytical model prediction of the overall variation of the PT force with gap opening angle is in good agreement with the test results.

The gap opening profile and position of neutral axis were measured during the test by an array of displacement transducers located along the depth of the beam at the beam-to-column interface. The gap opening profiles measured for three different values of gap opening angles in positive bending are presented in Fig. 12(a). The results confirm the linear variation of the gap opening across the beam depth, as assumed in the analytical model. The position of the neutral axis as a function of gap opening angle for positive bending is shown in Fig. 12(b). Again, the analytical model is in good agreement with the experimental results. For gap opening angles larger than 0.015 rad, the position of the neutral axis stabilizes at the inner side of the compression flange (29 mm from the top of the beam). This result confirms the assumption used in the analytical model to evaluate the forces in the system at the target rotation.

J. Struct. Eng. 2002.128:1111-1120.

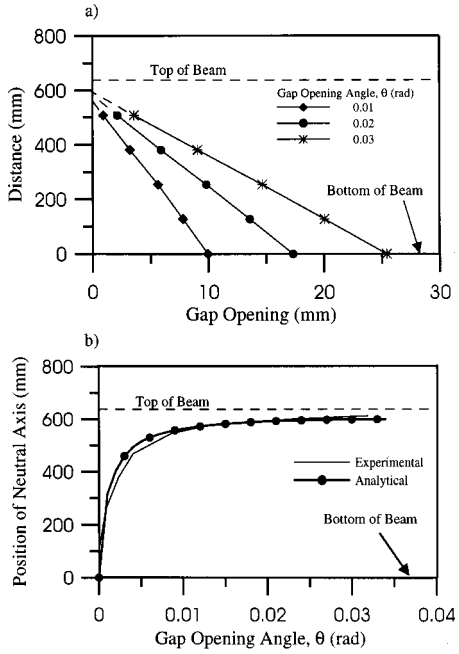

Fig. 12. Gap opening response of posttension energy dissipating connection (positive bending): (a) measured gap opening profile and (b) position of neutral axis

Two pairs of diagonal displacement transducers measured the shear strains in the panel zone of the column. The first pair of displacement transducers measured the shear strains in the lower part of the panel zone (between the PT bars and the bottom ED bars). The second pair of displacement transducers measured the shear strain across the entire panel zone (between the top and bottom ED bars). From these two measurements, the shear strains in the top part of the panel zone (between the top ED bars and the PT bars) could be obtained. Recall from Fig. 3 that the shear strains are not constant in the panel zone.

Fig. 13 presents the measured shear strains in the top and bottom parts of the panel zone as a function of the gap opening angle in negative bending. The shear strains in both parts of the panel zone increase with increasing gap opening angle. The two parts of the panel zone, however, experience significantly different values of shear strain. This result is consistent with the shear force distribution shown in Fig. 4. Under negative bending, the largest strains occur in the bottom part of the panel zone. Note also that the shear deformations in the top part of the panel zone remain almost constant after the ED bars have yielded, while the shear deformations in the bottom part of the panel zone continue to increase for larger values of gap opening angle.

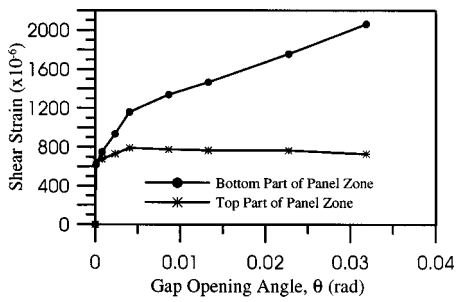

Fig. 13. Distribution of shear strains in column panel zone (negative bending)

Conclusions

A PTED moment connection for steel framed structures has been investigated analytically and experimentally. The PTED connection incorporates PT high-strength bars to provide a self-centering response along with ED bars that are able to yield in axial tension and compression. The analytical model developed is able to predict the moment-rotation relationship of a PTED connection. Based on this model, a simple design procedure for PTED connections has been developed. The results of a cyclic component test on the complete ED bar assembly showed that it was able to produce good energy dissipation characteristics for the PTED connections. Results of a cyclic test on a large-scale exterior beam-to-column joint showed that the proposed PTED connection is able to undergo large deformations with energy dissipation characteristics while keeping the beam and column undamaged and without residual drift. The results of the large-scale test also confirmed the adequacy of the analytical model and design procedure. Further analytical and experimental studies are required to understand more fully the seismic behavior of steel structures incorporating PTED connections of the type proposed in this study.

Acknowledgments

The financial assistance from the Dean's Office of the Irwin and Joan Jacobs School of Engineering at the University of Calif., San Diego in support of this research project is greatly appreciated. The in-kind support of Dywidag Systems International is also gratefully acknowledged. The writers express their gratitude to Roger Ferch, Vice President of Herrick Corporation, for his comments on the practical implementation of the proposed connection. Finally, the writers would like to acknowledge the invaluable support of the technical staff of the Powell Structures Laboratories during the experimental evaluation, especially that of Spyridon Kremmidas, Assistant Development Engineer at the University of California, San Diego.

References

American Institute of Steel Construction (AISC). (1993). *Load and resistance factor design specification for structural buildings*, American Institute of Steel Construction, Chicago.

American Institute of Steel Construction (AISC). (1997). *Seismic provisions for structural steel buildings*, American Institute of Steel Construction, Chicago.

Carr, A. J. (2000). "*RUAUMOKO*—Inelastic Dynamic Analysis Program." Dept. of Civil Engineering, Univ. of Canterbury, Christchurch, New Zealand.

Christopoulos, C., Filiatrault, A., and Folz, B. (2002). "Seismic response of self-centering hysteretic SDOF systems." *Earthquake Eng. Struct. Dyn.*, 31(5), 1131–1150.

Clark, P., Frank, K. Krawinkler, H., and Shaw, R. (1997). "Protocol for fabrication, inspection, testing, and documentation of beam-column tests and other experimental specimens." *Rep. No. SAC BD-97-02*, SAC Joint Venture, Sacramento, Calif.

El-Sheikh, M., Sause, R., Pessiki, S., Lu, L. W., and Kurama, Y. (1998). "Seismic analysis, behavior, and design of unbonded post-tensioned

J. Struct. Eng. 2002.128:1111-1120.

precast concrete frames.'' *PRESSS Rep. No. 98/04*, Lehigh Univ., Bethlehem, Pa.

Federal Emergency, Management Agency (FEMA). (2000). ''Recommended seismic design criteria for new steel moment frame buildings.'' *Rep. No. FEMA 350*, Federal Emergency Management Agency, Washington, D.C.

Gross, J. L., Engelhardt, M. D., Uang, C.-M., Kasai, K., and Iwankiw, N. R. (1999). ''Modification of existing welded steel moment frame connections for seismic resistance, design guide no. 12,'' American Institute of Steel Construction, Chicago.

Pampanin, S., Priestley M. J. N., and Sritharan, S. (1999). ''Frame direction modeling of the five-story PRESSS precast test building.'' *Rep. No. SSRP 99/20*, Univ. of California, San Diego.

Priestley, M. J. N. (1996). ''Seismic design philosophy for precast concrete frames.'' *Struct. Eng. Int. (IABSE, Zurich, Switzerland)*, 6(1), 25–31.

Priestley, M. J. N., Sritharan, S., Conley, J. R., and Pampanin, S. (1999). ''Preliminary results and conclusions from the PRESSS five-story precast concrete test building.'' *PCI J.*, 44(6), 42–67.

Priestley, M. J. N., and Tao, J. R. (1993). ''Seismic response of precast prestressed concrete frames with partially debonded tendons.'' *PCI J.*, 38(1), 58–67.

Ricles, J. M., Sause, R., Garlock, M. M., Peng, S. W., and Lu, L. W. (2000). ''Experimental studies on post-tensioned seismic resistant connections for steel frames.'' *Proc., STESSA 2000 Conference*, International Association of Steel Structures in Seismic Areas, Montreal, Canada, 231–238.

Ricles, J. M., Sause, R., Garlock, M. M., and Zhao, C. (2001). ''Posttensioned seismic-resistant connections for steel frames.'' *J. Struct. Eng.*, 127(2), 113–121.

SAC Steel Project (SAC). (1994). ''Proceedings of the invitational workshop on steel seismic issues.'' *Rep. No. SAC 94-01*, SAC Steel Project, Sacramento, Calif.

Shen, J., and Astaneh-Asl, A. (2000). ''Hysteresis model of bolted-angle connections.'' *J. Constr. Steel Res.*, 54, 317–343.

Shen, Q., and Kurama, Y. C. (2000). ''Lateral load behavior of unbonded post-tensioned hybrid coupled Walls.'' *Proc., 6th Int. Conf. on Steel-Concrete Composite Structures*, Los Angeles.

Stanton, J. F., Stone, W. C., and Cheok, G. S. (1997). ''Hybrid reinforced frame for seismic regions.'' *PCI J.*, 42(2), 20–32.

J. Struct. Eng. 2002.128:1111-1120.